Direct Measurement of Metal-Ion Chelation in the Active Site of the AAA$^+$ ATPase Magnesium Chelatase†

Joanne Viney,‡ Paul A. Davison,‡ C. Neil Hunter,‡ and James D. Reid*,§

Department of Molecular Biology and Biotechnology, University of Sheffield, Sheffield, United Kingdom S10 2TN and Department of Chemistry, University of Sheffield, Sheffield, United Kingdom S3 7HF

Received July 30, 2007; Revised Manuscript Received September 3, 2007

ABSTRACT: Magnesium chelatase catalyzes the first committed step in chlorophyll biosynthesis. This complex enzyme has at least three substrates and couples ATP hydrolysis to the insertion of Mg^{2+} into protoporphyrin IX. We directly observed metal-ion chelation fluorometrically, providing the first data describing the on-enzyme reaction. We describe the transient-state kinetics of magnesium chelatase with direct observation of the evolution of an enzyme−product complex $EMgD_{IX}$. We demonstrate that $MgATP^{2-}$ binding occurs after the rate-determining step. As nucleotide hydrolysis is essential for the overall reaction this must also occur after the rate-determining step. This provides the first evidence for the synchronization of the ATPase and chelatase pathways and suggests a mechanism where nucleotide binding acts to clamp the chelatase in a product complex. Comparison of rate constants for the slow step in the reaction with further transient kinetics under conditions where multiple turnovers can occur reveals that an additional activation step is required to explain the behavior of magnesium chelatase. These data provide a new view of the sequence of events occurring in the reaction catalyzed by magnesium chelatase.

Magnesium protoporphyrin IX chelatase (E.C. 6.6.1.1) catalyzes the insertion of a Mg^{2+} ion into protoporphyrin IX. This is the first committed step of (bacterio)chlorophyll biosynthesis. The minimum catalytic unit of magnesium chelatase contains three subunits, BchI/ChlI (38−42 kDa), BchD/ChlD (60−74 kDa), and BchH/ChlH (140−150 kDa), both in prokaryotes that produce bacteriochlorophyll *a* and in cyanobacteria and higher plants that synthesize chlorophyll *a* (*1*−*5*). An additional protein, Gun4, acts to activate magnesium chelatase in both cyanobacteria and higher plants (*6*−*8*). The I subunit is an ATPase (*9*, *10*), the D subunit forms a stable complex with the I subunit in the presence of Mg^{2+} and ATP (*9*, *11*), and the H subunit binds protoporphyrin IX as well as magnesium−protoporphyrin IX in the absence of the other magnesium chelatase subunits (*12*, *13*). An active magnesium chelatase can only be reconstituted by combining the individual subunits, but an HID complex has yet to be isolated. An HID complex is likely to be short lived, and many current models of magnesium chelatase action show obligatory subunit disassociation in every catalytic cycle (*14*−*16*). As subunit interactions are likely to be transient, analysis of the intact magnesium chelatase using enzyme kinetics holds a key to understanding both the assembly and the function of the complex.

The availability of purified recombinant subunits that comprise Mg chelatase from *Synechocystis* has allowed the most detailed kinetic and biochemical studies to date (*10*, *12*, *14*, *15*). Steady-state kinetics can provide valuable information regarding enzyme turnover rates and in some cases indicate the binding order of substrates in an enzyme-catalyzed reaction. However, they provide very little information on the transformations and conformational changes that occur as part of the catalytic cycle (*17*). The steady-state parameters are derived from an amalgam of multiple reactions occurring at the surface of the enzyme, and the individual reaction steps cannot be resolved in this way.

Recently, we performed the first detailed steady-state characterization of the intact magnesium chelatase from *Synechocystis* PCC6803 (*15*). The chelatase and ATPase reactions were shown to have a similar time course and the same lag phase, with the steady-state rates showing cooperative responses to magnesium. This work showed that approximately 14 ATP were hydrolyzed for every chelation under the assay conditions employed and confirmed the cooperative response of chelation activity to Mg^{2+} concentration. This cooperativity can be modulated by concentrations of both the porphyrin and nucleotide substrates.

Comparison of the steady-state kinetic parameters (*15*) with those previously obtained for the partial reactions of individual subunits shows that K_M^{MgATP} is substantially higher than in the isolated ChlI subunit, whereas K_M^{DIX} [1] of the intact chelatase is similar to the K_d^{DIX} of the HD_{IX} complex (*8*). Magnesium binding to the free ChlI subunit is not cooperative but allosterically coupled to the ATPase site. The significance of this information with respect to the on-enzyme catalytic steps cannot be assessed without transient kinetic studies.

Transient kinetic assays have been developed to directly observe metal-ion chelation, providing the first on-enzyme kinetic data. We directly observed the evolution of an

† Funded by the BBSRC (U.K.).

* To whom correspondence should be addressed: Phone: +44 114 222 29558. Fax: +44 114 222 9346. E-mail j.reid@sheffield.ac.uk.

‡ Department of Molecular Biology and Biotechnology.

§ Department of Chemistry.

[1] Abbreviations: D_{IX}, deuteroporphyrin IX; MgD_{IX}, magnesium-deuteroporphyrin IX; *I*, ionic strength.

10.1021/bi701515y CCC: $37.00
Published on Web 10/12/2007

Scheme 1: First Turnover Shifts the Enzyme from State I into a More Active Form (State II)[a]

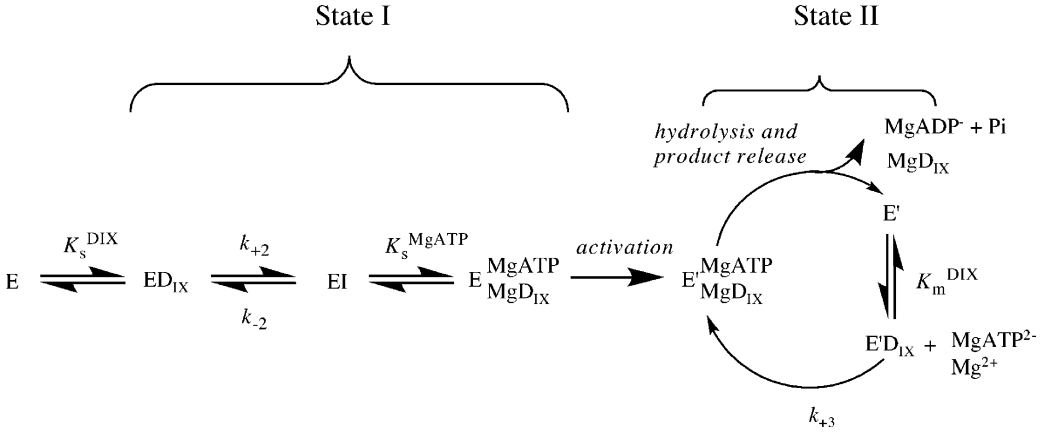

[a] K_m^{DIX} was estimated as 3.20 μM on the basis of steady-state data (*15*). Activation and in State II ATP hydrolysis and product release were presumed to be fast, and K_s^{DIX}, k_{+2}, k_{-2}, and K_s^{MgATP} were held constant at the values described above.

enzyme−product complex, $EMgD_{IX}$. The sequence of events occurring on the enzyme and leading to product formation has been revealed by these methods. In particular, we show that the rate-determining step occurs before nucleotide binding. Additionally, our data reveal that binding $MgATP^{2-}$ clamps the enzyme in a metalloporphyrin product complex, a key connection between the ATPase and the chelatase reaction cycles catalyzed by this enzyme. Comparison of rate constants for the slow step in the reaction with further transient kinetics under conditions where multiple turnovers can occur reveals that an additional activation step is required to explain the behavior of magnesium chelatase. This activation step reconciles the present transient kinetic study with the previous steady-state kinetics (*15*). In total, these data present a new view of the events occurring in the active site of magnesium chelatase where a slow reversible enzyme isomerization primes the system and metal-ion chelation is essentially irreversible after nucleotide binding. At relatively high porphyrin concentrations the first turnover promotes the enzyme into a more active state; this may provide an additional mechanism for controlling the flux into the chlorophyll biosynthetic pathway.

METHODS

Materials. Unless otherwise stated, chemicals were obtained from Sigma Chemical Co. (Poole, Dorset).

Protein Purification. The expression vectors pET9a-ChlI, pET9a-His_6ChlD, and pET9a-His_6ChlH (*2*) were used to produce combinant protein which was then purified as described previously (*2*, *15*).

Magnesium Chelatase Assay Conditions. Assay conditions were as described previously (*14*, *15*). Reactions were run at 34 °C, $I = 0.1$ or 0.15, and pH 7.7 in 50 mM MOPS/KOH, 0.3 M glycerol, and 1 mM DTT. Free metal-ion concentrations were controlled as described previously (*2*, *10*, *15*). Assays were initiated by addition of enzyme to give a final concentration as described in the figure legends. The subunit ratio was constant and has previously been shown to give an optimal enzyme activity (*14*). Enzyme subunits were incubated before the assay under conditions described in figure legends, but most data were collected with enzyme that was incubated for 30 min at 34 °C before the assay at 20 μM ChlH, 10 μM ChlI, 5 μM ChlD either with or without 5 mM $MgATP^{2-}$, and 10 mM Mg^{2+}. Substrate concentrations are given in the appropriate figures. Porphyrin solutions were made weekly in assay buffer and discarded if precipitated. ATP and ADP were determined spectrophotometrically, $\epsilon_{260} = 15\,400\ M^{-1}\ cm^{-1}$ (*18*), as was D_{IX}, $\epsilon_{398} = 433\,000\ M^{-1}\ cm^{-1}$, in 0.1 M HCl (*19*).

Fluorometric Detection of E.MgD$_{IX}$ Complexes. Reactions were followed fluorometrically on a SPEX Fluorolog spectrofluorometer. Fluorescence emission was detected at 580 nm with excitation at 295 nm. Emission was observed through a 515 nm band pass filter, and measurements were taken for 1 s every minute with the shutter closed between measurements.

Kinetic Data Analysis. Data were displayed in Igor Pro (Wavemetrics, Inc.) and fitted to the appropriate equation using nonlinear regression analysis. Simulations were carried out using KinSim (*20*). Characterizing parameters of the model in Scheme 1 were fit using numerical integration of the appropriate differential rate equations in Dynafit (*21*) to data collected with 8 μM ChlH, 4 μM ChlI, 2 μM ChlD, and 8 μM D_{IX}, 5 mM $MgATP^{2-}$, 10 mM Mg^{2+} in 50 mM MOPS/KOH, 0.3 M glycerol, 1 mM DTT, pH 7.7 at 34 °C, and $I = 0.1$.

RESULTS

Observation of the On-Enzyme Kinetics of Magnesium Chelatase. The complex reaction pathway of magnesium chelatase can be clarified by following the formation and loss of intermediate complexes along the reaction pathway. This requires an assay in which the enzyme is in large excess over porphyrin substrate so that single turnovers can be observed.

Fluorescence emission from enzyme-bound porphyrin was detected selectively following excitation of tryptophan residues. Photobleaching of the porphyrin was minimized using a shutter to reduce sample illumination. Following excitation at 295 nm, transient fluorescence was recorded from both the enzyme−substrate complex at 617 nm and the enzyme−product complex at 580 nm (Figure 1). This shows a decrease in the enzyme−substrate complex and the concomitant evolution of the $EMgD_{IX}$ complex and allows studies of the time-dependent formation and loss of enzyme−product and enzyme−substrate complexes.

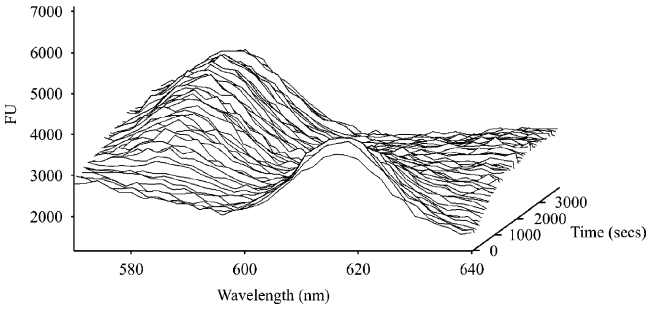

FIGURE 1: FRET reveals formation of enzyme-bound metalloporphyrin and depletion of enzyme−substrate complex in the reaction of magnesium chelatase. Assay contained *Synechocystis* ChlH (4 μM), ChlI (2 μM), and ChlD (1 μM), 5 mM $MgATP^{2-}$, 10 mM Mg^{2+} with 40 nM D_{IX}, in 50 mM MOPS/KOH, 0.3 M glycerol, 1 mM DTT pH 7.7 at 34 °C and $I = 0.1$.

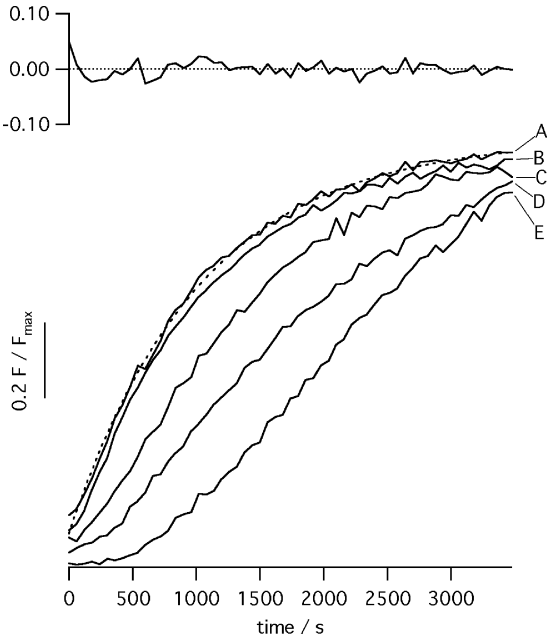

FIGURE 2: Preincubation of enzyme subunits removes the lag phase in product accumulation. Assays contained *Synechocystis* ChlH (2 μM), ChlI (1 μM), and ChlD (0.5 μM), 5 mM $MgATP^{2-}$, 10 mM Mg^{2+} with 40 nM D_{IX}, in 50 mM MOPS/KOH, 0.3 M glycerol, 1 mM DTT pH 7.7 at 34 °C and $I = 0.1$. Preincubation conditions were (A) 20 μM ChlH, 10 μM ChlI, 5 μM ChlD, this trace can be described by a single exponential, k_{obs} 0.001 s^{-1}, dashed line and residual; (B) 20 μM ChlH, 10 μM ChlI, 5 μM ChlD, 5 mM $MgATP^{2-}$, 10 mM Mg^{2+}; (C) separately 20 μM ChlH, 0.4 μM D_{IX} and 10 μM ChlI, 5 μM ChlD, 5 mM $MgATP^{2-}$, 10 mM Mg^{2+} combined in the assay; (D) 10 μM ChlI, 5 μM ChlD, 5 mM $MgATP^{2-}$, 10 mM Mg^{2+}. All preincubations were for 30 min at 34 °C. There was no preincubation for reaction E, which was started by adding enzyme directly to the assay. The scale bar shows a 20% change in fluorescence.

Elimination of Lag Phases To Permit Detailed Kinetic Analysis. Progress curves (Figure 2, trace E), collected using 295 nm excitation and recording emission at 580 nm, show substantial lag phases which cannot readily be fitted with sums of exponentials. Following earlier experience in separating enzyme activation from steady-state chelation (*14*), preincubation conditions were sought that would separate enzyme activation from metal-ion chelation. When ChlI and ChlD are allowed to form a complex (*14*) by preincubation with $MgATP^{2-}$ and Mg^{2+} (Figure 2, trace D) the lag is substantially reduced. Likewise an even shorter lag phase is seen (Figure 2, trace C) when, in addition, the porphyrin binding subunit, ChlH, is preincubated with deuteroporphyrin IX (D_{IX}). When all three subunits are preincubated with $MgATP^{2-}$ and Mg^{2+} (Figure 2, trace B) the lag phase is essentially eliminated and the trace can be described by a single exponential. We also demonstrate that the lag phase can be completely eliminated by incubation of all three subunits without any substrate (Figure 2, trace A). Preincubation conditions A and B were used throughout the work presented below and showed identical kinetics. Kinetic traces obtained after such preincubations (for example, Figure 2, trace A) can be described by a single-exponential function (Figure 2, dashed curve, and residual).

Observed Rate Constant for Enzyme−Product Complex Formation Depends on Enzyme Concentration. The observed rate constant for formation of an enzyme−product complex shows a hyperbolic dependence on enzyme concentration (Figure 3A). Preincubations of enzyme subunits with and without Mg^{2+} and $MgATP^{2-}$ give comparable data (Figure 3A, filled and open circles, respectively). The dependence of k_{obs} on enzyme concentration can be described by eq 1 with a negligible k_{-2}. The limiting rate constant k_{+2} is 2.4 $\times$ 10^{-3} s^{-1}, and K_s^{DIX} is 2.2 μM. This binding constant is estimated by assuming that the concentration of active sites in our enzyme preparation is the concentration of the ChlH subunit. This value agrees closely with the K_d^{DIX} obtained previously with the isolated ChlH subunit (*12*) and with the K_M^{DIX} obtained by steady-state kinetics in the study of the overall reaction (*15*). As porphyrin was in excess over binding sites for the previous two measurements, they rely on an accurate porphyrin concentration and not on the accurate determination of active-site concentration.

$$k_{obs} = \frac{k_{+2}}{1 + \frac{K_s^{DIX}}{[E]}} + k_{-2} \quad (1)$$

This behavior (Figure 3A) can, most simply, be described by a two-step mechanism with fast substrate binding followed by slower conversion of an enzyme−substrate complex to an enzyme−product complex (Figure 3D).

Observed Rate Constant for Enzyme−Product Complex Formation Depends on $MgATP^{2-}$ Concentration. The observed rate constant for formation of an $EMgD_{IX}$ complex decreases with increasing $MgATP^{2-}$ concentration (Figure 3B). As individual subunits of magnesium chelatase can catalyze ATP hydrolysis in the absence of porphyrin (*9*, *10*) subunits were preincubated without $MgATP^{2-}$ or Mg^{2+} before this series of assays. These data are consistent with the scheme shown in Figure 3E and can be described by eq 2 with characterizing parameters k_{+1} 2.3 $\times$ 10^{-3} s^{-1}, k_{-1} 4.2 $\times$ 10^{-3} s^{-1}, and K_s^{MgATP} at 62.3 μM. This results in an estimate for K_1, the equilibrium constant for the slow step (E to E′, k_{-1}/k_{+1}, in Figure 3E), of 1.82 $\pm$ 0.96.

$$k_{obs} = \frac{k_{-1}}{1 + \frac{[MgATP^{2-}]}{K_s^{MgATP}}} + k_{+1} \quad (2)$$

It is clear that the equilibrium constant for the slow step is only slightly unfavorable (i.e., $k_{-1} > k_{+1}$) and that this step

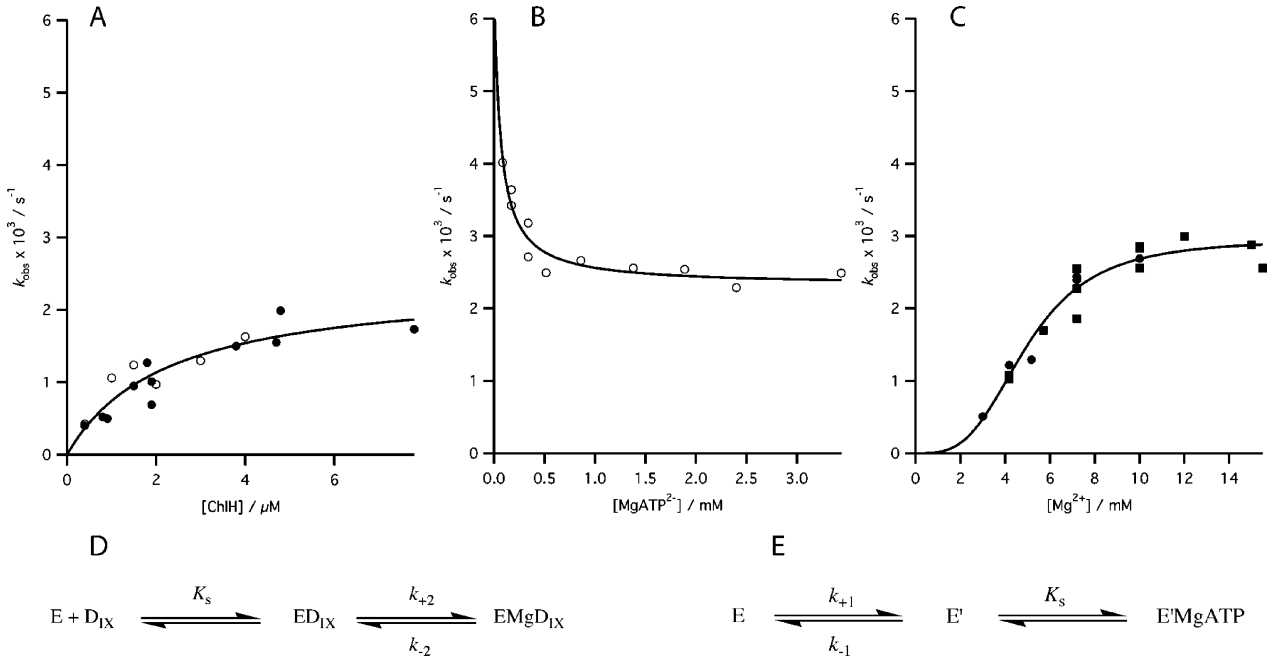

FIGURE 3: Observed rate constant for formation of enzyme−product complex depends on the concentration of enzyme and substrates. Assays contained 40 nM D_{IX}, in 50 mM MOPS/KOH, 0.3 M glycerol, 1 mM DTT, pH 7.7 at 34 °C and at $I = 0.1$ (circles) or $I = 0.15$ (squares) and when held constant 4 μM ChlH, 2 μM ChlI, 1 μM ChlD, 10 mM Mg^{2+}, and 5 mM $MgATP^{2-}$. Enzyme was incubated for 30 min at 34 °C before the assay at 20 μM ChlH, 10 μM ChlI, and 5 μM ChlD either with (filled circle, filled square) or without (open circle, open square) 5 mM $MgATP^{2-}$, 10 mM Mg^{2+}. (A) Assays contained varying enzyme concentration in the fixed ratio of 4H:2I:1D. The line is theoretical, described by eq 1, with characterizing parameters $k_{+2} = 2.40 \pm 0.31 \times 10^{-3}$ s^{-1} and $K_s^{DIX} = 2.24 \pm 0.65$ μM. (B) Assays contained varying $MgATP^{2-}$ concentrations. The theoretical line can be described by eq 2 with characterizing parameters $K_s^{MgATP} = 62.3 \pm 56.0$ μM and $k_{+1} = (2.32 \pm 0.12) \times 10^{-3}$ s^{-1}, $k_{-1} = (4.2 \pm 2.3) \times 10^{-3}$ s^{-1}. (C) Assays contained varying $MgCl_2$. The line can be described by eq 3 with characterizing parameters $k_{+1} = (2.95 \pm 0.15) \times 10^{-3}$ s^{-1}, $h = 3.33 \pm 0.59$, and $K_{0.5} = 4.96 \pm 0.24$ mM. (D) Scheme showing rapid binding of enzyme and porphyrin followed by slower metal-ion chelation. (E) Scheme showing slow enzyme isomerization followed by rapid binding of $MgATP^{2-}$. When the second step is much faster than the first then a single-exponential process will be observed, as described by eq 2.

is reversible. It is the binding of $MgATP^{2-}$ that drives this reaction to completion.

Dependence of the Rate of Formation of E.MgD$_{IX}$ on the Free Mg^{2+} Concentration. Assays at varying free Mg^{2+} concentration were carried out with 5 mM $MgATP^{2-}$ at two ionic strengths, $I = 0.1$ (Figure 3C, circular symbols) as in previous work (*10*, *15*) and $I = 0.15$ (Figure 3C, square symbols). The higher ionic strength allowed clearly saturating concentrations of Mg^{2+} to be used. Data collected at the higher ionic strength show a sigmoid trend and can be described by the Hill equation (eq 3).

$$k_{obs} = \frac{k}{1 + \left(\frac{K_{0.5}}{[Mg^{2+}]}\right)^h} \quad (3)$$

The limiting rate constant, k, was 2.9×10^{-3} s^{-1} with a $K_{0.5}$ of 5.0 mM and h of 3.3.

Reconciling Rate Constants from Steady-State and Transient-State Kinetic Data. The data presented above lead to a view where the slowest first-order step leading to formation of an EP complex has a rate constant of ca. 2.6×10^{-3} s^{-1}. This is approximately five times slower than k_{cat}, determined previously to be 13×10^{-3} s^{-1} on the basis of steady-state data (*15*). These two data sets were collected under quite different concentration regimes, here with enzyme in excess over porphyrin and previously with porphyrin in excess (*15*). In order to test this discrepancy and the possibility that k_{cat} had been overestimated in the previous study, a reaction was set up with a high porphyrin concentration (8 μM) and a final enzyme concentration (8 μM ChlH, 4 μM ChlI, 2 μM ChlD) above K_s^{DIX} (2.2 μM, Figure 3A). The resulting time course is shown in Figure 4 (filled circles). Simulation of the model in Figure 3D was performed using the kinetic parameters deduced from the data shown in Figure 3A with the assumption that the enzyme concentration is 8 μM (Figure 4; right-hand trace). This does not agree with the experimental data. If there had been a 5-fold underestimation of the active enzyme, which would reconcile the single-turnover data with previous steady-state data, then there would be 40 μM enzyme present. Simulation of these conditions is illustrated in the central trace in Figure 4, which also does not explain these data. A numerical error in k_{cat} therefore does not provide an explanation for the discrepancy between the k_{cat} from the steady-state data and the rate constant from the transient kinetic data.

An alternative model was tested where the first turnover promotes the enzyme into a more active form (Scheme 1). With the assumption that activation is fast and irreversible and holding the kinetic parameters for the less active form to those determined above, this model provides good agreement with the data (Figure 4, left-hand trace) with k_{+3} 0.013 ± 0.0005 s^{-1}. This value is identical to k_{cat} determined previously (*15*). The binding constant between porphyrin substrate and the activated enzyme is not well defined by these data (Figure 4), and it is not appropriate to attempt to obtain fitted values for this parameter. This is a consequence of the experimental design where both [E] and [S] $\gg K_d$.

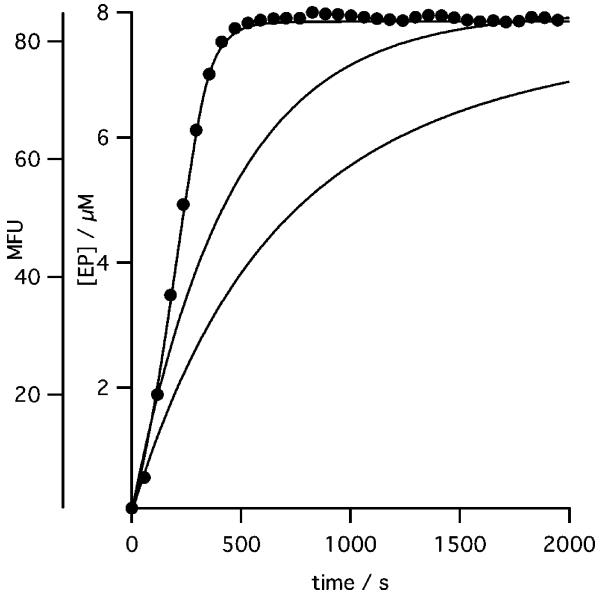

FIGURE 4: Fluorescence time course (λ_{ex} 295 nm, λ_{em} 580 nm) of the reaction of *Synechocystis* magnesium chelatase (ChlH 8 μM, ChlI 4 μM, ChlD, 2 μM) with 8 μM D_{IX}, 5 mM $MgATP^{2-}$, 10 mM Mg^{2+} in 50 mM MOPS/KOH, 0.3 M glycerol, 1 mM DTT, pH 7.7 at 34 °C and $I = 0.1$. Filled circles represent the experimental data. The lines are theoretical and can be described by (right and central traces) Figure 3D with characterizing parameters $K_s^{DIX} = 2.2$ μM, $k_{+2} = 2.2 \times 10^{-3}$ s^{-1}, assuming 8 μM active enzyme (right trace) or 40 μM active enzyme (central trace). The fitted line through the experimental data (left trace) assumes a model where the first turnover activates the enzyme, Scheme 1, with 8 μM active enzyme and $k_{+3} = 0.013 \pm 0.0005$ s^{-1}.

This binding constant is likely to be perturbed by competition for metaloporphyrin product, especially as the K_d values of the isolated ChlH subunit complexes with D_{IX} and MgD_{IX} are similar (*12*). While the K_d value for the isolated ChlH−D_{IX} complex, the K_m for D_{IX} in the overall reaction of magnesium chelatase, i.e., state II (*15*), and the *K* determined here for the ED_{IX} complex in state I are similar, product binding to the intact enzyme has not been measured and may be significantly different than that observed with the isolated porphyrin binding subunit. The likely validity of the hypothesis presented in Scheme 1 and the implications for our understanding of the magnesium chelatase mechanism are discussed below.

DISCUSSION

Magnesium chelatase is a particularly tractable member of the AAA+ superfamily as the ATPase activity is coupled to large spectroscopic changes in the active site. These spectroscopic signals offer a novel opportunity to detect site−site communication in the AAA+ superfamily. All previous investigations of this enzyme as well as most previous investigation of the AAA+ enzymes have relied on a steady-state description of the catalytic cycle. In this paper we report on the events occurring in the active site of this AAA+ enzyme; this work complements previous detailed description of other members of the AAA+ superfamily including clamp loaders (*22*, *23*) and proteases (*24*−*27*).

Magnesium chelatase is a complex enzyme, coupling the hydrolysis of around 14 $MgATP^{2-}$ to the insertion of a Mg^{2+} ion into a porphyrin ring. The high stoichiometry and cooperative response to free Mg^{2+} leads to complex steady-state kinetics (*15*). As the overall reaction catalyzed by magnesium chelatase is complex, observing single steps should provide a clearer understanding of the reaction. Our data provide the first evidence for synchronization of the ATPase and chelatase pathways and shows that nucleotide binding acts to clamp the chelatase in a product complex.

Complex Formation and Enzyme Activation. Magnesium chelatase catalyzed reactions frequently show a lag phase in product production, and these have often been attributed to subunit assembly (*14*, *28*). When prepared from chloroplasts the enzyme disassociates into components during isolation (*28*), and the conditions needed to restore activity are similar to those required to assemble a functional magnesium chelatase from pure recombinant subunits (*13*, *14*). As recombinant subunits are produced separately they have to be combined to form the active enzyme; this process is aided by the presence of substrates (*14*). It is not unusual for the assembly of oligomeric enzymes to be slow at the low protein concentrations suitable for steady-state assays.

Magnesium chelatase shows a pronounced lag phase in the steady state. This hysteresis can be reduced, but not entirely eliminated, by incubating the enzyme with a partial set of substrates (*13*, *14*). In contrast, with enzyme in excess of porphyrin the lag phase can be eliminated by incubating all three subunits at high concentration (Figure 1). Our data are in broad agreement with that seen earlier (*14*), although this is the first observation of a preincubation without $MgATP^{2-}$ eliminating the lag. This preincubation was carried out at protein concentrations 20 times those used previously (*14*). If formation of active enzyme in the lag period is promoted by, but does not absolutely depend upon, the presence of $MgATP^{2-}$, then high protein concentrations will drive formation of active enzyme even in the absence of $MgATP^{2-}$.

It is worth noting that lag phases arise when the reactions occurring in the lag are distinctly slower than those that occur later. Thus, slow assembly reactions that cause the lag phase will not occur in every catalytic cycle.

Nucleotide Binding and Metal-Ion Chelation. The transient kinetics of magnesium chelatase show a remarkably diverse set of responses to reactant concentration (Figure 3). Nevertheless, these are consistent and can be used to produce an integrated model for the chelation reaction. Notably, in all three cases the limiting observed rate constants at saturating enzyme or substrate are essentially identical. We therefore argue that these reflect the same reaction step and that the chelation step in Figure 3D and the isomerization step in Figure 3E are equivalent. Two models are consistent with these observations (Scheme 2A and B); these models differ in the nature of the intermediate. This is either an enzyme substrate complex that is primed for metal-ion chelation (Scheme 2A) or an enzyme product complex (Scheme 2B). In both cases nucleotide binding acts to clamp the chelatase in a metalloporphyrin product complex.

The models illustrate the role of $MgATP^{2-}$ binding in the chelation mechanism but do not reveal the role of nucleotide hydrolysis. Binding, not necessarily hydrolysis, of $MgATP^{2-}$ is a key step in driving formation of an enzyme−metalloporphyrin complex.

$MgATP^{2-}$ hydrolysis is not included in our model (Scheme 2) as the background activity of the chelatase (*9*) makes it

Scheme 2: Reaction Pathway of Magnesium Chelatase in the Presence of Saturating Mg^{2+} [a]

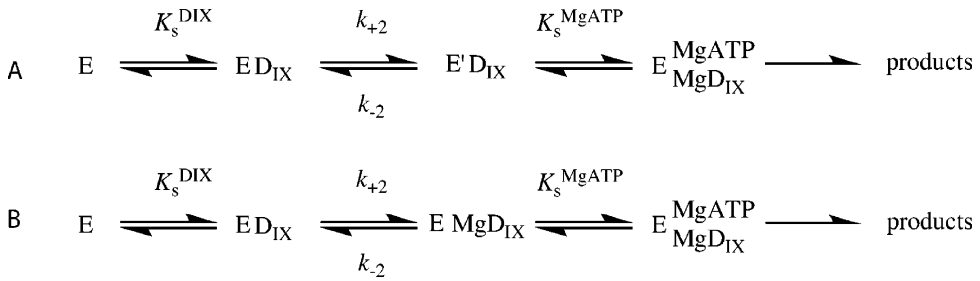

[a] $K_s^{DIX} = 2.24 \pm 0.65\ \mu M$, $K_s^{MgATP} = 62.3 \pm 56.0\ \mu M$, $k_{+2} = 0.0023 \pm 0.0012\ s^{-1}$, $k_{-2} = 0.0042 \pm 0.0023\ s^{-1}$ and product release is fast.

unfeasible to measure the coupled activity under our reaction conditions.

The slow step in this scheme is either isomerization that primes the enzyme for chelation (Scheme 2A) or metal-ion chelation (Scheme 2B). This step is reversible with an equilibrium constant of 1.82 ± 0.96 and broadly favors enzyme-bound porphyrin substrate (ED_{IX}). Binding of $MgATP^{2-}$ (K_s^{MgATP} = ca. 60 μM) shifts this equilibrium toward metalloporphyrin products; $MgATP^{2-}$ thus clamps the enzyme in a metalloporphyrin complex. Our data show this shift in equilibrium constant directly. When $MgATP^{2-}$ is saturating (Figure 3A) the intercept of the k_{obs} curve is essentially zero, demonstrating that the slow step is irreversible. We have no information on events occurring after formation of an enzyme−product complex, and it will be of great interest to determine how nucleotide hydrolysis and metalloporphyrin release are coupled. Product release was not observed, e.g., by a decrease in signal from the EP complex. This implies that either product release is fast enough not to be observed or enzyme concentration is high enough for the EP complex to dominate. In practice, previous steady-state data at low enzyme concentrations (*15*) showed multiple turnovers, suggesting that product release, from enzyme in state II, is fast.

Magnesium Cooperativity. Placing a mechanistic interpretation on cooperative Mg^{2+} binding is beyond the scope of our data; the model above (Scheme 1) applies to Mg^{2+}-saturated forms of the enzyme. Our data do not support models of cooperativity where Mg^{2+} binding drives subunit assembly to form a more active enzyme state, as roughly the same extent of cooperativity is seen here at high enzyme concentration ($h = 3.3 \pm 0.59$) as was seen previously in the steady state ($h = 3.3 \pm 0.9$ (*15*)) when all substrates were saturating. A full model, with explicit Mg^{2+} binding, will be complex.

Magnesium Chelatase Has Two Distinct Activity States. The limiting first-order rate constant observed under enzyme in excess conditions is roughly five times smaller than that inferred from steady-state measurements. This can occur if the reaction follows different pathways at high and low substrate concentration or if one of the measurements is incorrect. Our data (Figure 4) strongly suggest that magnesium chelatase follows different reaction pathways when enzyme saturates porphyrin as opposed to when porphyrin is saturating enzyme (Scheme 1) and that the difference in rate constants cannot be attributed to an overestimation of k_{cat}.

While other reasonable models need to be explored, our data can be explained by magnesium chelatase having two distinct activity states with relatively slow turnover in state I serving to promote the enzyme into a more active state II. In the steady state, when magnesium chelatase is undergoing multiple turnovers state II predominates (Scheme 1), whereas when the chelatase is in excess only single turnovers occur and the characteristics of state I can be explored. The data presented here, and summarized in Scheme 2, provide a detailed characterization of state I of magnesium chelatase. Steady-state kinetics, carried out under conditions where state II predominates (*15*), are informative but cannot reveal the interconversion of enzyme forms. It remains to be established if the nucleotide clamp described above in the state I system is also a feature of the enzyme in state II. Biologically, switching betweens states I and II may provide an additional mechanism to control flux into the chlorophyll biosynthetic pathway.

ACKNOWLEDGMENT

We thank Mrs. S. McLean for technical support.

REFERENCES

1. Gibson, L. C. D., Willows, R. D., Kannangara, C. G., von Wettstein, D., and Hunter, C. N. (1995) Magnesium-protoporphyrin chelatase of *Rhodobacter sphaeroides*: reconstitiution of activity by combining the products of the *bchH*, *-I* and *-D* genes expressed in *Escherichia coli*, *Proc. Natl. Acad. Sci. U.S.A. 92*, 1941−1944.
2. Jensen, P. E., Gibson, L. C. D., Henningsen, K. W., and Hunter, C. N. (1996) Expression of the *chlI*, *chlD*, and *chlH* genes from the cyanobacterium *Synechocystis* PCC6803 in *Escherichia coli* and demonstration that the three cognate proteins are required for magnesium-protoporphyrin chelatase activity, *J. Biol. Chem. 271*, 16662−16667.
3. Petersen, B. L., Jensen, P. E., Gibson, L. C. D., Stummann, B. M., Hunter, C. N., and Henningsen, K. W. (1998) Reconstitution of an active magnesium chelatase enzyme complex from the *bchI*, *D* and *H* gene products of the green sulphur bacterium *Chlorobium vibrioforme* expressed in *E. coli*, *J. Bacteriol. 180*, 699−704.
4. Papenbrock, J., Grafe, S., Kruse, E., Hanel, F., and Grimm, B. (1997) Mg-chelatase of tobacco: identification of a Chl D cDNA sequence encoding a third subunit, analysis of the interaction of the three subunits with the yeast two-hybrid system, and reconstitution of the enzyme activity by co-expression of recombinant CHL D, CHL H and CHL I, *Plant J. 12*, 981−990.
5. Gibson, L. C. D., Marrison, J. L., Leech, R. M., Jensen, P. E., Bassham, D. C., Gibson, M., and Hunter, C. N. (1996) A putative Mg chelatase subunit from *Arabidopsis thaliana* cv C24. Sequence and transcript analysis of the gene, import of the protein into chloroplasts, and in situ localization of the transcript and protein, *Plant Physiol. 111*, 61−71.
6. Davison, P. A., Schubert, H. L., Reid, J. D., Iorg, C. D., Heroux, A., Hill, C. P., and Hunter, C. N. (2005) Structural and biochemical characterization of Gun4 suggests a mechanism for its role in chlorophyll biosynthesis, *Biochemistry 44*, 7603−7612.
7. Verdecia, M. A., Larkin, R. M., Ferrer, J. L., Riek, R., Chory, J., and Noel, J. P. (2005) Structure of the Mg-chelatase cofactor GUN4 reveals a novel hand-shaped fold for porphyrin binding, *PLoS Biol. 3*, e151.

8. Larkin, R. M., Alonso, J. M., Ecker, J. R., and Chory, J. (2003) GUN4, a regulator of chlorophyll synthesis and intracellular signaling, *Science 299*, 902−906.
9. Jensen, P. E., Gibson, L. C. D., and Hunter, C. N. (1999) ATPase activity associated with the magnesium-protoporphyrin IX chelatase enzyme of *Synechocystis* sp. PCC6803: evidence for ATP hydrolysis during Mg2+ insertion, and the MgATP-dependent interaction of the ChlI and ChlD subunits, *Biochem. J. 339* (Pt 1), 127−134.
10. Reid, J. D., Siebert, C. A., Bullough, P. A., and Hunter, C. N. (2003) The ATPase activity of the ChlI subunit of magnesium chelatase and formation of a heptameric AAA+ ring, *Biochemistry 42*, 6912−6920.
11. Gibson, L. C. D., Jensen, P. E., and Hunter, C. N. (1999) Magnesium chelatase from *Rhodobacter sphaeroides*: initial characterization of the enzyme using purified subunits and evidence for a BchI-BchD complex, *Biochem. J. 337* (Pt 2), 243−251.
12. Karger, G. A., Reid, J. D., and Hunter, C. N. (2001) Characterization of the binding of deuteroporphyrin IX to the magnesium chelatase H subunit and spectroscopic properties of the complex, *Biochemistry 40*, 9291−9299.
13. Willows, R. D., and Beale, S. I. (1998) Heterologous expression of the *Rhodobacter capsulatus BchI*, *-D*, and *-H* genes that encode magnesium chelatase subunits and characterization of the reconstituted enzyme, *J. Biol. Chem. 273*, 34206−34213.
14. Jensen, P. E., Gibson, L. C. D., and Hunter, C. N. (1998) Determinants of catalytic activity with the use of purified I, D and H subunits of the magnesium protoporphyrin IX chelatase from Synechocystis sp. PCC6803, *Biochem. J. 334* (Pt 2), 335−344.
15. Reid, J. D., and Hunter, C. N. (2004) Magnesium-dependent ATPase Activity and Cooperativity of Magnesium Chelatase from Synechocystis sp. PCC6803, *J. Biol. Chem. 279*, 26893−26899.
16. Axelsson, E., Lundqvist, J., Sawicki, A., Nilsson, S., Schroder, I., Al-Karadaghi, S., Willows, R. D., and Hansson, M. (2006) Recessiveness and dominance in barley mutants deficient in Mg-chelatase subunit D, an AAA protein involved in chlorophyll biosynthesis, *Plant Cell 18*, 3606−3616.
17. Hoggins, M., Dailey, H. A., Hunter, C. N., and Reid, J. D. (2007) Direct Measurement of Metal Ion Chelation in the Active Site of Human Ferrochelatase, *Biochemistry 46*, 8121−8127.
18. Dawson, R. M. C. (1969) *Data for biochemical research*, 2nd ed., Oxford University Press, New York.
19. Falk, J. E. (1964) *Porphyrins and metalloporphyrins*, Elsevier, London.
20. Barshop, B. A., Wrenn, R. F., and Frieden, C. (1983) Analysis of numerical methods for computer simulation of kinetic processes: development of KINSIM−a flexible, portable system, *Anal. Biochem. 130*, 134−145.
21. Kuzmic, P. (1996) Program DYNAFIT for the analysis of enzyme kinetic data: application to HIV proteinase, *Anal. Biochem. 237*, 260−273.
22. Bertram, J. G., Bloom, L. B., Hingorani, M. M., Beechem, J. M., O'Donnell, M., and Goodman, M. F. (2000) Molecular mechanism and energetics of clamp assembly in *Escherichia coli*. The role of ATP hydrolysis when gamma complex loads beta on DNA, *J. Biol. Chem. 275*, 28413−28420.
23. Smiley, R. D., Zhuang, Z., Benkovic, S. J., and Hammes, G. G. (2006) Single-molecule investigation of the T4 bacteriophage DNA polymerase holoenzyme: multiple pathways of holoenzyme formation, *Biochemistry 45*, 7990−7997.
24. Martin, A., Baker, T. A., and Sauer, R. T. (2005) Rebuilt AAA + motors reveal operating principles for ATP-fuelled machines, *Nature 437*, 1115−1120.
25. Hersch, G. L., Burton, R. E., Bolon, D. N., Baker, T. A., and Sauer, R. T. (2005) Asymmetric interactions of ATP with the AAA+ ClpX6 unfoldase: allosteric control of a protein machine, *Cell 121*, 1017−1027.
26. Vineyard, D., Zhang, X., and Lee, I. (2006) Transient kinetic experiments demonstrate the existence of a unique catalytic enzyme form in the peptide-stimulated ATPase mechanism of *Escherichia coli* Lon protease, *Biochemistry 45*, 11432−11443.
27. Vineyard, D., Patterson-Ward, J., and Lee, I. (2006) Single-turnover kinetic experiments confirm the existence of high- and low-affinity ATPase sites in *Escherichia coli* Lon protease, *Biochemistry 45*, 4602−4610.
28. Walker, C. J., and Weinstein, J. D. (1994) The magnesium-insertion step of chlorophyll biosynthesis is a two-stage reaction, *Biochem. J. 299* (Pt 1), 277−284.

BI701515Y